Journal of Engineering and Architecture
June 2019, Vol. 7, No. 1, pp. 30-38
ISSN: 2334-2986 (Print), 2334-2994 (Online)

Published by American Research Institute for Policy Development
DOI: 10.15640/jea.v6n2a4
URL: https://doi.org/10.15640/jea.v6n2a4

Comparative Study of Moment-Curvature Diagram in Beams with FRP Bars for Three Constitutive Models of the Concrete

Mag Daniel Quiun Wong[1] **, Mag Johan Hinostroza Yucra**[2]

Abstract

It is widely known the problem of corrosion that affects the steel bars used in reinforced concrete. For example, in 2012 India spent 70.3 billion dollars with a GDP of 1670 billion on structures that suffered corrosion, in other words 4.2% of GDP (Gerhardus et al 2016). Also, the cost of corrosion in USA in 2016 was 2.5 trillion dollars (nace.org/publications/Cost-of-Corrosion-Study / G2MT). For this reason, it is necessary to continue making studies related to mitigation of corrosion. Recently, the basalt bars have appeared as an alternative reinforcement to steel bars in concrete. The advantage of basalt bars over the steel bars lies in that they do not suffer corrosion. These basalt bars are the fusion of basalt fibers from the rock and resin. The aim of this paper is to analyze the behavior of a concrete beam cross section, reinforced with basalt bars through the moment-curvature diagram. Then, the comparison of three moment-curvature diagrams obtained with different constitutive models available for concrete is presented. The constitutive models selected for the purposes of this paper have been proposed by the American Concrete Institute (ACI), the European Concrete Committee (CEB) and Kent and Park, for the calculation of the nominal bending moment.

Keywords: FRP bars; moment-curvature; constitutive models; basalt bars

Introduction

Commonly, the reinforcement used when designing concrete sections is steel rebars. However, as environmental conditions affect these materials, alternative materials are needed that offer comparative advantages, such as fiber reinforced polymers (FRP). The design of beams reinforced with these bars is governed by the ACI 440 regulation, which also includes some recommendations to be applied during construction. This paper presents an analysis of these elements through the moment-curvature diagrams, using three constitutive concrete models that overcome the limitations of the compression block of the ACI with respect to the elaboration of the diagram.

1. Reinforced Polymers with Fibers (FRP)

An FRP bar is a set of filaments or fibers that are in a binder matrix of polymeric resin and are classified according to the type of fiber they have, such as glass (GFRP), carbon (CFRP), basalt (BFRP) or aramid (AFRP) according to Gremel, D (2003). Among the main advantages that can be noted of FRP bars compared to steel bars are: Anisotropic material, high resistance to corrosion, non-magnetic, high strength / specific weight, lower maintenance cost, repair and / or structural rehabilitation (Quake Wrap 2017). Figure 1 shows the constitutive diagrams of the steel and some FRP bars.

[1]Professor of Civil Engineer of PUCP, Perú, dquiun@pucp.edu.pe
[2]Assistant Professor of PUCP, Perú, johan.hinostroza@pucp.edu.pe

It can be noticed that the deformations reached in the FRP bars are smaller than in the steel and that its stress-strain relation is totally linear without the presence of a yield platform which could lead to the possibility of fragile failure. However, from the values shown in Table 1, it can be noted that the ultimate stress for the FRP bars are greater than for the steel, which will mean a greater reserve of resistance.

Table 1.-Mechanical properties of FRP bars and steel (Adapted from ACI 440, 2006)

Material	Last Effort (MPa)	Elastic Modulus (GPa)	Deformation of failure (%)
GFRP	483-1600	35-51	1.2-3.1
CFRP	600-3690	120-580	0.5-1.7
AFRP	1720-2540	41-125	1.9-4.4
STEEL	483-690	200	6-12

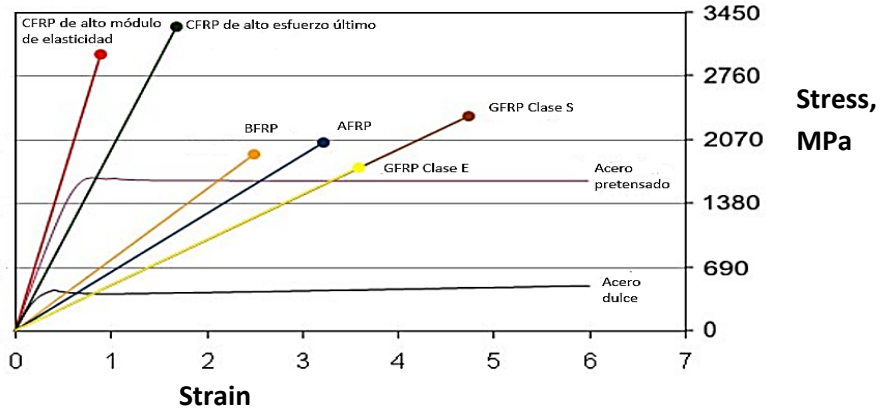

Fig. 1.-Graphs stress vs. Strain of FRP and Steel bars (Adapted from Prince Engineering 2011)

2. Constitutive Models of the Concrete

A constitutive model is a diagram that aims to describe the stress-strain behavior of a given material. The constitutive models selected for the purposes of this article have been those proposed by the American Concrete Institute (ACI), the European Concrete Committee (CEB) and Kent and Park, referred to the calculation of the nominal bending moment. However, only the last two will be used for the moment-curvature diagram and the first will be used taking into account certain observations.

2.1 American Concrete Institute (ACI)

In this model, the actual stress diagram in the concrete is replaced by an equivalent compression block that is defined by two parameters: "α" and "β". The first parameter is the ratio of the stress in the block to the resistance in compression of the concrete f'c; and the second, the relation between the depth of the compression block of stresses with respect to the neutral axis of the section. A value of 0.85 is usually accepted for α, while the values adopted for β are dependent on the value of the compressive strength of the concrete (De la Fuente 2007). This model facilitates the calculation of the nominal moment.

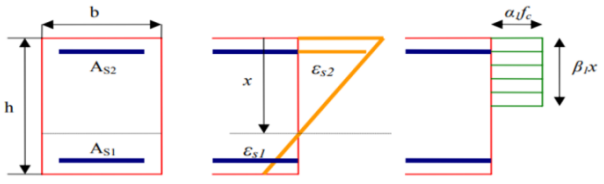

Fig. 2 –Rectangular equivalent block (Adapted from De la Fuente 2007)

2.2 European Concrete Committee (CEB)

This model is used in Europe, corresponds to a perfectly plastic inelastic model. The stress diagram consists of a second degree parabolic curve with the final vertex corresponding to a concrete deformation equal to 0.002; and then, a straight line whose end corresponds to a concrete deformation equal to 0.0035. For both vertices, the other component is equal to the compressive strength of the concrete reduced to a value of 0.85 f'c (Ottazzi, 2017).

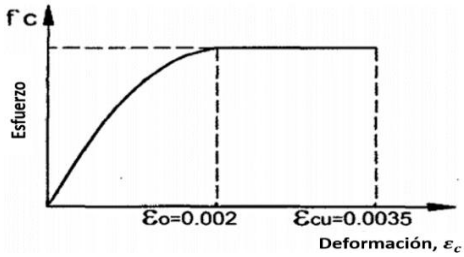

Fig. 3–Parabolic-rectangle model CEB (Adapted from Ottazzi, 2017)

2.3 Kent and Park

This model has among its parameters the volumetric volume of confinement, so it can represent the behavior of concrete with or without confinement. It has an initial parabolic zone that reaches the compressive strength of the concrete f'c at a unit strain equal to 0.002, then follows a linear decreasing zone until it loses capacity by 80%, whose deformation is defined corresponding to a loss of 50% capacity. When it comes to confined concrete, after losing capacity by 80%, the model considers a constant remaining capacity valid until exhaustion (Chang 2015).

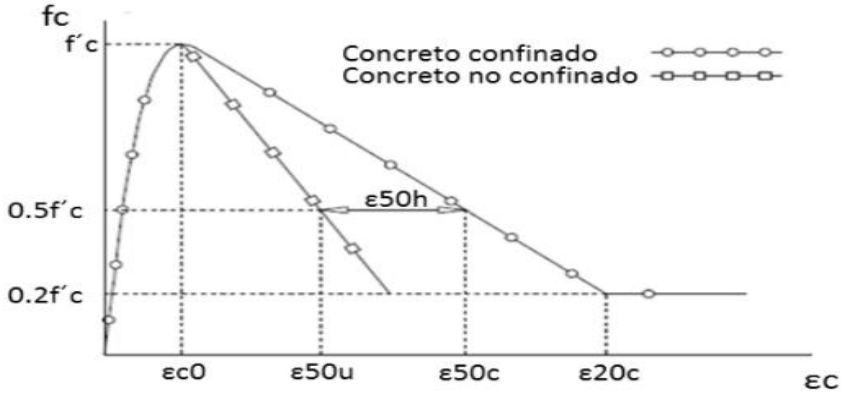

Fig. 4 – Parabolic-lineal model Kent-Park (Chang 2015)

The deformation when losing 50% capacity in an unconfined concrete (ε50u) is defined by Eq.[1], where f'c is expressed in psi. On the other hand, in the case of confined concrete, the deformation increases up to a value of ε50c by the presence of stirrups (ε50h) which is defined by Eq. [2], ϱ is the volumetric quantity of confining stirrups as a function of the confined core, *b* is the smallest dimension of the confined core and *s* is the spacing between stirrups.

$$\varepsilon 50u = (3 + 0.002\, f'c)/(f'c - 1000) \quad [1]$$

$$\varepsilon 50h = 0.75\, \varrho\, (b/s)^{0.5} \quad [2]$$

3. Calculation Nominal Moment

Actually, the Strength Design is used, which is governed by the premise "Design Resistance ≥ Required Resistance" where the Design Resistance is the nominal resistance reduced by the factor φ corresponding to the required internal force and the Required Resistance comes from increased loads by factors indicated in ACI (Ottazzi 2017). Then, the calculation of the nominal moment for the 3 constituent models presented in the previous section is presented.

This will be done (Fig. 5) for a rectangular section of 25x50cm with reinforcement of 3 bars of 3/4" (A_f=8.52 cm²), the concrete has a compression strength f'c=210 kg/cm², the elastic module of the reinforcement is E_f=570000 kg/cm² and the ultimate tensile stress in the reinforcement is f_{fu}=12000 kg/cm²

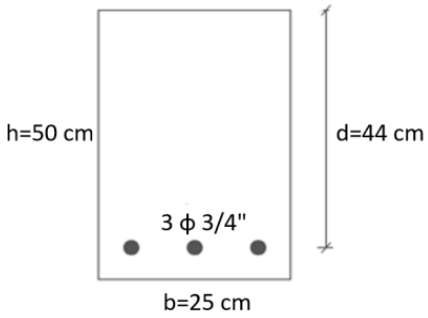

Fig. 5– Beam section considered for calculations (Own source)

3.1 American Concrete Institute (ACI)

The nominal moment calculation according to the ACI 440.1R is performed according to the value of the reinforcement ratio (ρ_f), if it is greater or less than the ratio of balanced reinforcement (ρ_{fb}). The equations to find the value of the ratios are presented in [3] and [4]; then, the nominal moment calculation is presented according to the criteria mentioned above:

$$\rho_f = \frac{A_f}{bd} \quad [3]$$

$$\rho_{fb} = 0.85\,\beta_1 \frac{f'_c}{f_{fu}} \frac{E_f \varepsilon_{cu}}{E_f \varepsilon_{cu} + f_{fu}} \quad [4]$$

Nominal Moment for $P_F > P_{FB}$

ACI proposes, first, to calculate the reinforcement stress (f_f), which must be less than the last reinforcement stress. Through the equilibrium of forces and the compatibility of deformations, expressions [5] to [8] can be obtained. The difference is that one takes into account the reinforcement area, while the other expression is based on the ratio of reinforcement whose calculation is expressed in Eq. [3]

$$f_f = \sqrt{\frac{(E_f \varepsilon_{cu})^2}{4} + \frac{0.85\beta_1 f'_c}{\rho_f} E_f \varepsilon_{cu}} - 0.5 E_f \varepsilon_{cu} \leq f_{fu} \quad [5]$$

$$M_n = A_f f_f \left(d - \frac{a}{2}\right) \quad [6]$$

Where:

$$a = \frac{A_f f_f}{0.85 f'_c b} \quad [7]$$

It also applies:

$$M_n = \rho_f f_f \left(1 - 0.59 \frac{\rho_f f_f}{f'_c}\right) b d^2 \quad [8]$$

Nominal Moment for $P_F < P_{FB}$

In this case, the failure of the element starts with the breaking of the FRP reinforcement, so an equivalence must be established so that the concrete stress corresponds to the deformation that has been reached, which probably does not coincide with the maximum deformation that concrete can reach (0.003). When the unknowns are the deformation of the concrete at the failure (ε_c), the depth of the neutral axis (c), the reduction factor for the block (α) and the ratio of the depth of the block with respect to the neutral axis (β), the ACI440 proposes that the nominal moment be approximately eq. [9]:

$$M_n = A_f f_{fu} \left(d - \frac{\beta_1 c}{2}\right) \quad [9]$$

Although it does not influence the calculation of the nominal moment, it may be interesting to mention that the resistance reduction factor ϕ varies according to the reinforcement ratio used as shown in Figure 6:

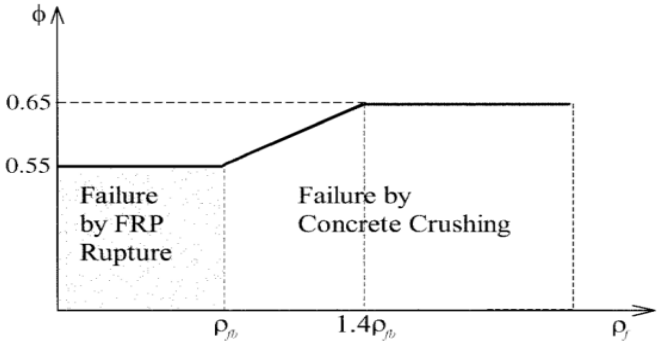

Fig. 6– Variation of the value of ϕ with the amount of reinforcement (ACI 440, 2006)

Considering a ultimate deformation of concrete (ε_{cu}) of 0.003, which is the one corresponding to the idealization of the compression block, and applying Eq. [3] and [4] we have: $\rho_f = 0.00775$; $\rho_{fb} = 0.00158$. The condition $\varrho_f > \varrho_{fb}$ is fulfilled, so that from Eq. (5), (7) and (6) it may be obtained: $f_f = 49955\ N/cm^2$; $a = 9.54\ cm$; $M_n = 167\ kN.m$

3.2European Concrete Committee (CEB)

In this case, the calculation of the nominal moment is based on the compatibility of deformations, stress-strain relation and equilibrium in the section (Fig. 7). It is important to point out that it will not be sought to verify the yield condition, as it is done when the reinforcement is steel, since the stress-strain relation for the FRP bars is linear elastic for any deformation up to the failure.

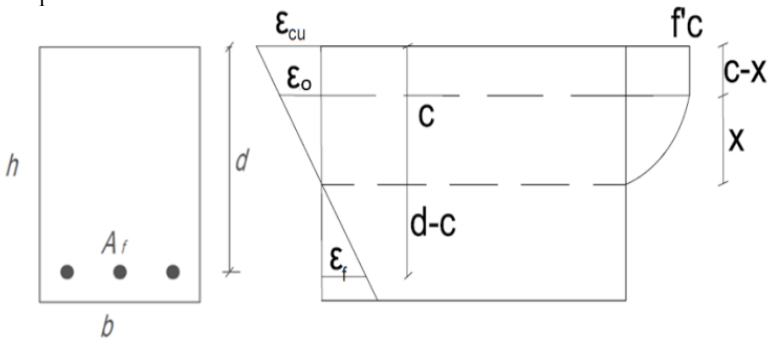

Fig. 7– Deformations in the section of the beam (Own source)

It will be necessary to take into account during the calculations, the difference of equations in the shape of the concrete curve since the initial part is parabolic and the final part is linear. The equations obtained will be given by Eq. [10] to [18]:

Compatibility: $\varepsilon_f = \frac{\varepsilon_{cu}}{c} * (d - c)$ [10]

Stress-strain relations: $f_f = E_f * \varepsilon_f$ [11]

Balance of the section: $T = A_f * f_f$ [12]

$C_c = \frac{2}{3} * f'c * b * c * \frac{\varepsilon_o}{\varepsilon_{cu}} + f'c * b * c * (1 - \frac{\varepsilon_o}{\varepsilon_{cu}})$ [13]

$C_c = T$ [14]

Parabolic part length: $x = \frac{\varepsilon_o}{\varepsilon_{cu}} * c$ [15]

Compression centroid: $\underline{y} = \frac{\frac{2}{3} * f'c * x * (c - x + \frac{3x}{8}) + f'c * (c-x)^2/2}{\frac{2}{3} * f'c * x + f'c * (c-x)}$ [16]

Lever arm: $j_d = d - \underline{y}$ [17]

Nominal moment: $M_n = j_d * f_f * A_f$ [18]

If Eq. (12) is replaced in Eq. (11) and then placed next to Eq. (13) in Eq. (14), the value of c can be obtained.

$$c = 11.42\ cm$$

With the value of c, we can obtain the length of the parabolic part by means of Eq. (15) and then replace it in Eq. (16) and find the centroid of the compressions in the concrete. With Eq. (17), the lever arm of either force can be determined, either the tension in the reinforcement or the compression in the concrete. Finally, Eq. (10), (11) and (18) are used to find the nominal moment.

$$x = 6.53\ cm \quad \bar{y} = 4.75\ cm$$
$$j_d = 39.25\ cm$$
$$\varepsilon_f = 0.009985$$
$$f_f = 56915\ N/cm^2$$
$$M_n = 190.3\ kN.m$$

3.3 Kent and Park

In this case, the process is similar to that presented in the calculation of the nominal moment with the constitutive diagram proposed by the CEB. The values to be obtained are that the final deformation in the concrete that reaches a value of 0.004 and that the final part is a straight line with a fall of 0.15 f'c which triggers that the last compression stress considered for concrete is 0.85f 'c; therefore, the parts will be parabolic and trapezoidal. The equations are conserved except those in which the geometry of the constitutive diagram influences, such as Eq. (13) and (16), of which their corrections will be presented next in [19], [20] and [21]:

$f_u = 0.85f'c$ [19]

$C_c = \frac{2}{3} * f'c * b * c * \frac{\varepsilon_o}{\varepsilon_{cu}} + (f'c + f_u) * 0.5 * b * c * (1 - \frac{\varepsilon_o}{\varepsilon_{cu}})$ [20]

$\underline{y} = \frac{\frac{2}{3}*f'c*x*\left(c-x+\frac{3x}{8}\right)+f_u*\frac{(c-x)^2}{2}+(f'c-f_u)*\frac{(c-x)^2}{3}}{\frac{2}{3}*f'c*x+(f'c+fu)*0.5*(c-x)}$ [21]

Following the process presented above, we can find:

$$c = 12.17\ cm;\ x = 6.09\ cm;\ \underline{y} = 5.32\ cm;\ j_d = 38.68\ cm;\ \varepsilon_f = 0.01046;\ f_f = 59632\ N/cm^2$$
$$M_n = 196.5\ kN.m$$

4. Moment-Curvature Diagram

The moment-curvature diagram is a way to describe the behavior of a section of concrete with reinforcement. The points commonly used for the preparation of this diagram are those corresponding to the cracking moment of the section (Mcr), start of the yield of the reinforcement (My) and the maximum capacity of the section (Mmax). Nevertheless, FRP bars do not have a yield platform. For this reason, in the present case, the moment-curvature diagram omits the point corresponding to the start of yielding of the reinforcement (My).

The calculation of the moments before and immediately after the cracking with the selected constitutive models are carried out under the same process; also the following hypotheses are considered (Ottazzi 2017): 1) The flat sections remain flat; 2) The behavior of concrete, under service loads, in tension and compression has an elastic linear behavior, this approach is conservative for compression stress up to 0.4 or 0.5 of f'c; 3) There is no possibility of a failure occurring prematurely by shear or by lateral buckling; and 4) The bond between the concrete and the bars FRP is perfect. The procedure to calculate the moment before the cracking (M_v), with the contribution of the concrete and the FRP bars, is done using the moment of inertia of the transformed section (I_{tr}) and the flexural tensile strength of concrete (f_r), which is given in ec. [22] and [23]:

$$f_r = 2\sqrt{f'_c} \quad [22]$$

$$M_v = f_r I_{tr} \quad [23]$$

The calculation of stress in the concrete can be done based on the bending moment (M), to the position of the neutral axis (c) and to the moment of inertia of the transformed section. In turn, with this value we can calculate the curvature reached, see Eq. [24] and [25].

$$fc = \frac{M*c}{I_{tr}} \quad [24] \qquad \varphi = \frac{\varepsilon_c}{c} = \frac{\frac{fc}{Ec}}{c} \quad [25]$$

The results of the moment-curvature calculation are presented, moments before the Cracking (AF) and instants after cracking (DF) are obtained for section, AF transformed cracked and for DF, of the cracked transformed section ignoring the concrete in tension; for both cases, the process of calculating the other intermediate variables is common: M is obtained through Eq. (23); c is obtained from the static moment sum with respect to the upper edge; is calculated using Eq. (24) and to find Eq. (25) is used. The results obtained for the 3 constituent models that are common to all, are shown in Table 2, the reason is that they are governed by the hypothesis that the concrete behavior will be linear as long as the stress is less than 0.5f'c.

Table 2 –Values obtained from the calculation for before and after the cracking common to the 3 constitutive models of concrete

	$I_{tr}(cm^4)$	$M\ (kN.m)$	$c\ (cm)$	$fc\ (N/cm^2)$	$\varphi\ (1/m)$
AF	525728	61.2	25.10	292.2	0.0005
DF	35631	63.7	5.83	1041.5	0.0082

4.1 Moment-Curvature of the beam with reinforcing steel.

For a matter of interest, the procedure for the moment curvature relation has been developed for the same cross section of the beam, using reinforced steel bars. The constitutive model proposed by the European Concrete Committee was used (CEB). For the calculation of the necessary points for the construction of the moment-curvature diagram, the previously explained procedures were followed. Nevertheless, due to the fact that the steel has a yield zone, an additional calculation was made corresponding to the moment and curvature at the beginning of yield of the steel. The calculation of moment of yielding was performed based on deformation compatibility, stress-strain relationship. It will be necessary to take into account during the calculations the different equations in the shape of the curve of the concrete, since the initial part is parabolic, and the final part is linear. The equations obtained will be those shown [26] to [33]:

- Compression in concrete:

$$fc = -a_1 {\varepsilon_c}^2 + a_2 \varepsilon_c \quad [26]$$

$$a_1 = f'c/{\varepsilon_o}^2 \quad [27]$$

$$a_2 = 2f'c/\varepsilon_o \quad [28]$$

- Result of compressions in the concrete:

$$C_c = \int_0^c fc(y)\,bdy = b(0.5 \times a_2 \times c \times \varepsilon_c - a_1/3 \times c \times {\varepsilon_c}^2 \quad [29]$$

- Resultant from steel tractions: $T = A_s f_y$ [30]
- Compatibility: $\frac{\varepsilon_c}{c} = \frac{\varepsilon_y}{(d-c)}$ [31]
- Creep curve and creep moment:

$$\varphi_y = \frac{\varepsilon_c}{c} \quad [32]$$

$$My = T(d - k_2 c) \quad [33]$$

The results obtained by solving Eq. [26] through Eq. [33] are illustrated in figs. 8 and 9:

$$fc = 121.6\frac{Kg}{cm^2}\ c = 10.99\,cm\ \ \varepsilon_c = 0.0007\ \varphi_y = 6.39\ \times 10^{-3}\frac{1}{m}\ \ My = 14.35\ Ton - m$$

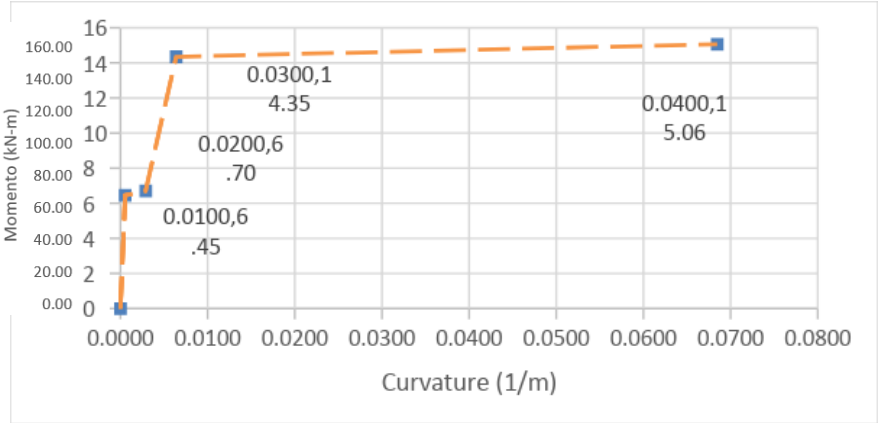

Fig. 8- Moment-Curvature diagram for the beam with reinforcing steel (Own image)

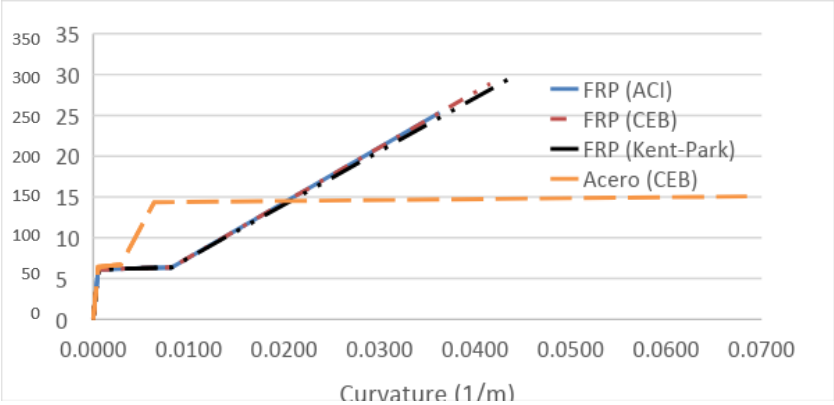

Fig. 9- Moment-Curvature diagram of beams reinforced with FRP and steel (Own image)

The 3 moment-curvature diagrams elaborated with FRP reinforcement do not present a significant difference. This is logical because the first two break points were calculated under the hypothesis of a linear behavior of the stress in the concrete, so got the same values. As for the final point, it is the one that corresponds to the moment nominal value, all these values do not differ considerably, being the value of ACI more conservative. In addition, in the moment-curvature diagram with steel reinforcement, we have 3 breakpoints, from the second one to the last one the line is practically a constant value.

5. Ductility of the Reinforced Beam with Steel and FRP

The ductility of a material is defined as the amount of maximum plastic deformation that is able to support a material before breaking. The equation to obtain this ductility is presented in Eq. [34].

$$\mu\varphi = \frac{\varphi_{máx}}{\varphi_y} \qquad [34]$$

First, the important points of the moment-curvature diagram are presented of the beam with steel reinforcements, to obtain the ductility of the element. The steel presents a point at which yield begins, which is fundamental to perform this calculation. Applying Eq. [34] with the data from table 3, we obtain $\mu\varphi = 10.72$. Second, or the beam reinforced with FRP bars, the ductility was calculated by establishing that the curvature of yield is obtained with similar values for steel. This assumption is not correct since the FRP bars do not have a yield platform, so this is somewhat an indicator adopted to obtain the curvature ductility and thus, establish some relevant conclusions regarding this (Table 4).

Table 3 – Breaking points of the bending moment for the beam with reinforcing steel

BEAM WITH STEEL		
	Moment (kN.m)	**Curvature (1/m)**
Before cracking	64.5	0.0005
After cracking	67.0	0.0029
Start creep	143.5	0.0064
Nominal	150.6	0.0685

Table 4 –Breaking points of the bending moment for the FRP beam reinforcement beam

FRP		
	Moment (kN.m)	**Curvature (1/m)**
Before cracking	61.2	0.0005
Assumed for point of creep in reinforcement	63.1	0.0064
After cracking	63.7	0.0082
Nominal	288.9	0.0416

Applying Eq. (34) with the data that can be extracted from table 6, we obtain: $\mu\varphi = \frac{0.0416}{0.0064} = 6.51$

6. Conclusions

The nominal moments, the maximum peaks in the moment-curvature diagram for FRP bars, are quite similar to each other, being the value calculated with the equations from the ACI the most conservative one. The last deformations considered in the concrete vary according to the adopted constitutive model and this must be taken into account during the calculations. In addition, by superimposing the moment-curvature diagrams the differences between them is not significant. The lack of a yield platform for FRP bars makes it impossible to find a moment of yielding and its corresponding curvature. In order to quantitatively assess the ductility, the assumption was made to adopt the yield of steel as if it also occurred in the FRP bars. A lower curvature ductility was obtained in this case. These results are dependent on factors such as the section analyzed, as there is less ductility, the possibility of a fragile failure grows.

References

ACI Committee 440. (2006). ACI 440.1R-6 Guide for the design and construction of structural reinforced with FRP.

De la Fuente, A. D. A. (n.d.). Análisis no lineal y comportamiento en servicio y rotura de secciones construidas evolutivamente sometidas a flexocompresión. Retrieved January 2, 18, UPC.

Gremel, D. G. (n.d.). Fiber Reinforced Polymer (FRP) Reinforcing Bar. Nova Award Nomination 4. Retrieved December 28, 17, from < http://www.cif.org/noms/2003/04_-_FRP_Reinforcing_Bar.pdf

Koch, G. K. (2016). International Measures of Prevention, Application, and Economics of Corrosion Technologies Study. Houston, Texas, USA: Gretchen Jacobson, NACE.

Prince Engineering. (n.d.). FRP reinforcement for structures. Retrieved December 29, 2017, from http://www.build-on-prince.com/frp-reinforcement.html

Quake Wrap. (n.d.). Ventajas de Quake Wrap-Materials FRP. Retrieved December 28, 2017, from http://www.quakewrap.com/esp/advantages.php

Ottazzi, G. (2017). Apuntes del curso de Concreto Armado 1 (15th ed.). Lima, Perú: Pontificia Universidad Católica del Perú.